

Molecular dynamics simulation of crystal dissolution from calcite steps

N. H. de Leeuw* and S. C. Parker†

School of Chemistry, University of Bath, Claverton Down, Bath BA2 7AY, United Kingdom

J. H. Harding‡

Department of Physics and Astronomy, University College London, Gower Street, London WC1E 6BT, United Kingdom

(Received 22 March 1999)

Molecular-dynamics simulations were used to model two stepped $\{10\bar{1}4\}$ surfaces of the calcium carbonate polymorph calcite. The acute monatomic steps were found to be more stable than the obtuse monatomic steps. The initial stages of dissolution from the steps were considered *in vacuo* and in water. *In vacuo* CaCO_3 was shown to dissolve preferentially from the obtuse step. In aqueous environment both stepped surfaces are stabilized by the presence of the water molecules although the relative stabilities remain similar. Using potential parameters that reproduce experimental enthalpies of the dissolution of calcite crystal, the formation of the double kinks on the obtuse step is shown to cost less energy than dissolution from the acute step, probably due to the lower stability of the obtuse surface. The simulations suggest that formation of the kink sites on the dissolving edge of the obtuse step of calcite is the rate determining step and this edge is predicted to dissolve preferentially, which is in agreement with experimental findings of calcite dissolution under aqueous conditions. [S0163-1829(99)12039-3]

INTRODUCTION

Calcite is one of the most abundant minerals in the environment and of fundamental importance in many fields, both inorganic and biological. It is a building block of shells and skeletons¹ and is used as a carbon isotope counter in marine carbonates, with a view to assessing the relationship between the CO_2 -induced greenhouse effect and climate.² Furthermore, calcium carbonate is important in ion exchange, due to its strong surface interactions with heavy metals in the environment,^{3,4} in energy storage where the products of its endothermic decomposition into CaO and CO_2 can be stored and subsequently reacted exothermically to re-release the energy⁵ and in industrial water treatment.⁶ Hence, calcite has been the subject of extensive and varied research. One area of research, which has attracted much attention is crystal growth and dissolution, e.g., Refs 7–10. As the concentration of calcium carbonate in many natural waters exceeds the saturation level, the precipitation of calcite in industrial boilers, transportation pipes and desalination plants is of concern¹¹ and it is therefore important to learn how crystal growth and dissolution are affected and modified. Often studies have concentrated on the incorporation in the crystal of foreign ions such as copper and manganese,¹² iron¹³ and other divalent cations,^{14–16} phosphate species,^{6,17} or organic matter.^{18–20} Alternatively, side reactions like the oxidation of pyrite and ammonia affect the rate of CaCO_3 dissolution.²¹ Earlier computational studies^{22,23} have confirmed experimental findings²⁴ that lithium and HPO_4^{2-} impurities radically change the morphology of calcite, and predicted that magnesium ions would do likewise, which was later confirmed by Compton and Brown¹⁴ who found that magnesium ions inhibit calcite growth.

The $\{10\bar{1}4\}$ surface is by far the most stable plane of calcite and dominates the observed morphology.^{25–27} Hence,

it has been the subject of many investigations, both in ultra-high vacuum such as the scanning electron microscopy (SEM) study by Goni, Sobrado, and Hernandez,²⁸ in air²⁹ and under aqueous conditions such as the atomic force microscopy (AFM) investigations by Ohnesorge and Binnig³⁰ and Liang *et al.*³¹ However, no experimental surface is truly planar and there are always defects present like steps and kinks. Indeed, calcite growth is found to occur through steps³² and spiral dislocations,³³ often in monolayers from the step as observed by Liang *et al.*³¹ in their AFM study of the calcite $\{10\bar{1}4\}$ plane under aqueous conditions and by Stipp, Gutmannsbauer, and Lehmann²⁹ who used scanning force microscopy (SFM) to study the same surface in air over some days and found the steps to spread one layer at a time. Foreign ions can be incorporated at the growing steps, e.g., boron oxyanions.³⁴ Recent models of step dissolution have included a terrace-ledge-kink model, successfully describing the initial stages of pit growth on the $\{10\bar{1}4\}$ surface,^{35,36} and a kinetic Monte Carlo model which reproduces experimental pit-growth behavior.³⁷ In addition, atomistic simulation methods have been used to model growth inhibition by incorporation of diphosphates into the steps³⁸ although they did not explicitly include solvent effects.

The aim of the work described in this paper is to use molecular-dynamics simulations to investigate the energetics of key stages in calcite dissolution, which is achieved by modelling the dissolution of CaCO_3 units from two different monatomic steps on the $\{10\bar{1}4\}$ surface. In addition to studying calcium carbonate removal from the steps in vacuum, we have extended our study to include the effect of water on the stepped surfaces to begin to understand the influence of aqueous conditions on the growth and dissolution process.

THEORETICAL METHODS

The surface and adsorption energies of the calcite surfaces were modeled using classical molecular dynamics simula-

tions. These are based on the Born model of solids,³⁹ which assumes that the ions in the crystal interact *via* long-range electrostatic forces and short-range forces, including both the repulsions and the van der Waals attractions between neighbouring electron charge clouds. The short-range forces are described by simple analytical functions that need to be tested using, for example, electronic structure calculations. The electronic polarisability of the ions is included *via* the shell model of Dick and Overhauser⁴⁰ in which each polarizable ion, in our case the oxygen ion, is represented by a core and a massless shell, connected by a spring. The polarizability of the model ion is then determined by the spring constant and the charges of the core and shell. When necessary, angle-dependent forces are included to allow directionality of bonding as, for example, in the model of the covalent carbonate anion developed by Pavese *et al.*⁴¹

The computer code used for the molecular-dynamics simulations was DL_POLY 2.9.⁴² To obtain the necessary data on bulk liquid water we simulated a box containing 256 water molecules at a temperature of 300 K. The equilibration of the water simulation cell was achieved by initially setting the experimental density of $\rho = 1.0 \text{ g/cm}^3$ and using constant number of particles, volume, and energy (NVE), constant temperature (NVT) and constant pressure and temperature (NPT) ensembles in sequence. The final data collection simulations were run at NPT. The stepped calcite surfaces were modeled as a repeating calcite slab, containing 120 CaCO_3 units and a void and run using the NVT ensemble. Water molecules were then introduced in the void and the whole system including solvent molecules was again simulated under NVT conditions. The simulation cell, consisting of calcite slab and 48 water molecules, contained 1152 species including shells.

In the DL_POLY code the integration algorithms are based around the Verlet leap-frog scheme⁴³ and we used the Nosé-Hoover algorithm^{44,45} for the thermostat as this algorithm generates trajectories in both NVT and NPT ensembles thus keeping our simulations consistent. The Nosé-Hoover parameters were set at 0.5 for both the thermostat and barostat relaxation times (ps). There are two ways of treating the shells which are essentially massless; either performing an energy minimization of shells only at each timestep⁴⁶ or assigning a small mass to the shells.^{47,48} The latter is the approach used by DL_POLY. We chose 0.2 a.u. for the oxygen shell, which is small compared to the mass of the hydrogen atom of 1.0 a.u. This ensured that there would be no exchange of energy between vibrations of oxygen core and shell with oxygen and hydrogen vibrations.⁴⁹ However, due to the small shell mass we needed to run the molecular-dynamics (MD) simulation with a small timestep of 0.2 femtoseconds in order to keep the system stable.

The surface energy is a measure of the thermodynamic stability of the surface with a low, positive value indicating a stable surface. It is given by

$$\gamma = \frac{U_s - U_b}{A}, \quad (1)$$

where U_s is the energy of the surface block of the crystal, U_b is the energy of an equal number of atoms of the bulk crystal, and A is the surface area. The energies of the blocks are

the sum of the energies of interaction between all atoms, which are comprised of long-ranged Coulombic interactions and short-ranged terms. The latter are described by parameterized analytical expressions.

We used the parameters for the short-range interactions derived empirically by Pavese *et al.*⁴¹ in their study of the thermal dependence of structural and elastic properties of calcite. Although this potential model was fitted to bulk properties, it is generally possible for ionic materials to transfer potential parameters to surface calculations. In semiconductors, where the surface involves breaking bonds, and metals where the surface means a sudden change in the electron density, there is often a problem with transferability from bulk potential parameters to surfaces. However, in ionic materials after relaxation, the Madelung potentials are 90% or more of the bulk values and hence the change of ionic radii is negligible. Oliver *et al.*,⁵⁰ for example, used bulk derived potentials for their computational study comparing to scanning tunnelling microscopy results of WO_3 surfaces, and found excellent agreement between calculations and experiment. Since the surfaces considered in this work leave the carbonate group intact the bulk derived potential model will be adequate. The parameters used for the intra- and intermolecular water interactions are those described in a previous paper of MD simulations on MgO surfaces.⁴⁹ We used the potential parameters previously fitted to calcite for the interactions between water molecules and calcium carbonate surfaces.⁵¹ This previous study of hydrated calcite surfaces reproduced experimental 1×1 surface symmetry and structural features of the $\{10\bar{1}4\}$ surface and comparable surface relaxation of the $\{10\bar{1}1\}$ surface. The same potential parameters were then used successfully in our study comparing the surface structures and stabilities of the calcium carbonate polymorphs aragonite and vaterite with calcite.⁵²

RESULTS

Calcite has a rhombohedral crystal structure with space group $R\bar{3}c$ and $a = b = 4.990 \text{ \AA}$, $c = 17.061 \text{ \AA}$, $\alpha = \beta = 90^\circ$, and $\gamma = 120^\circ$.⁵³ On energy minimization the structure relaxed to $a = b = 4.797 \text{ \AA}$, $c = 17.482 \text{ \AA}$, $\alpha = \beta = 90^\circ$, and $\gamma = 120^\circ$. As we were interested in calcite dissolution from steps on the dominant $\{10\bar{1}4\}$ surface, we studied the $\{31\bar{4}8\}$ and $\{3\bar{1}\bar{2}16\}$ vicinal surfaces, which each contain $\{10\bar{1}4\}$ planes and monatomic steps. The sides of the steps are also $\{10\bar{1}4\}$ surfaces and the step edges of the two stepped surfaces are identical to the two different edges of the calcite rhomb [Fig. 1(a)]. The steps on the $\{31\bar{4}8\}$ surface are acute, i.e., the carbonate group on the edge of the step overhangs the plane below the step [Fig. 1(b)] and the angle between step wall and plane is 80° on the relaxed surface [cf. exp. 78°].⁴ For brevity we will refer to this surface as the A surface. The steps on the $\{3\bar{1}\bar{2}16\}$ surface on the other hand are obtuse, i.e., the carbonate groups on the step edge lean back with respect to the plane below [Fig. 1(c)] with an angle between step wall and plane of 105° on the relaxed surface [exp. 102°].⁴ We will refer to this surface as the O surface. These two types of steps are found experimentally to form the dissolving edges of etch pits^{4,35} and the obtuse step is found to be the fastest moving of the two.

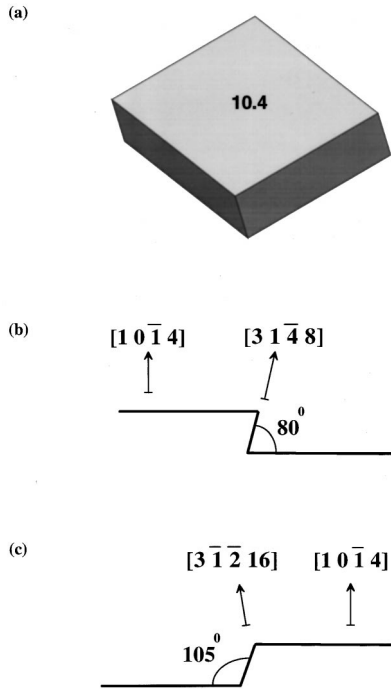


FIG. 1. (a) Equilibrium morphology of calcite showing acute and obtuse edges, schematically represented in (b) acute edges on the $\{3\bar{1}48\}$ surface, and (c) obtuse edges on the $\{3\bar{1}216\}$ surface.

PURE SURFACES

We first considered the two unhydrated stepped surfaces. The surface energies are collected in Table I from which can be seen that the *A* surface ($\gamma=0.35 \text{ Jm}^{-2}$) is more stable than the *O* surface ($\gamma=0.68 \text{ Jm}^{-2}$), cf. $\gamma=0.05 \text{ Jm}^{-2}$ for the very stable flat $\{10\bar{1}4\}$ surface under the same conditions. The difference between the surface energies of the two steps is probably due to the different relaxation of the two steps. The carbonate group on the acute step rotates into the edge, increasing its bonding and smoothing the edge to a much larger extent than the obtuse step. Table I also gives the surface energies where consecutive calcium carbonate units have been removed from the steps (one unit=25%). As can be seen, removing one or more units from the steps and hence introducing kink sites on the edge^{35,54} does not have a large effect on the relative surface energies and hence, thermodynamic stabilities of the pure surfaces, although the full steps (0% and 100%) are somewhat more stable. When a second calcium carbonate unit (50%) is removed from the step, this can be taken from two possible sites, (i) either next to the first empty site, where no additional kink sites are introduced or (ii) the second calcium carbonate unit is re-

TABLE I. Surface energies of unhydrated calcite surfaces.

| Surface | Surface energies of unhydrated calcite surfaces (Jm^{-2}) | | | | | |
|----------------------------|--|------|------------------|------------------|------|------|
| | 0% | 25% | 50% ^a | 50% ^b | 75% | 100% |
| <i>A</i> $\{3\bar{1}48\}$ | 0.35 | 0.38 | 0.41 | 0.44 | 0.42 | 0.35 |
| <i>O</i> $\{3\bar{1}216\}$ | 0.68 | 0.72 | 0.71 | 0.72 | 0.68 | 0.68 |

^aAdjacent calcium carbonate units removed.

^bAlternating configuration, forming crenellated edge.

TABLE II. Energies of removing calcium carbonate units from unhydrated calcite surfaces.

| Surface | Dissolution energies of unhydrated calcite surfaces/ CaCO_3 unit removed (kJ mol^{-1}) | | | | |
|----------------------------|--|------------------|------------------|-------|-------|
| | 25% | 50% ^a | 50% ^b | 75% | 100% |
| <i>A</i> $\{3\bar{1}48\}$ | +68.5 | +57.6 | +76.9 | +42.8 | +16.0 |
| <i>O</i> $\{3\bar{1}216\}$ | +58.4 | +21.0 | +34.3 | +1.3 | -1.3 |

^aAdjacent calcium carbonate units removed.

^bAlternating configuration, forming crenellated edge.

moved isolated from the first empty site introducing twice the number of kink sites and resulting in a crenellated edge. From the surface energies for these half grown steps, it can be seen that for both steps, but especially the *A* surface, the configuration with two adjacent calcium carbonate units removed is more stable and hence this position is preferred over the configuration where the calcium carbonate units are alternating along the steps.

The dissolution energy, neglecting hydration, is defined as the average energy per calcium carbonate unit to remove n units from the step as follows:

$$E_{\text{dts}} = \frac{E_{\text{dissolvedstep}} - (E_{\text{fullstep}} + n\text{CaCO}_3)}{n}, \quad (2)$$

where the energy of the CaCO_3 is taken as the lattice energy. The dissolution energies are given in Table II. The fully dissolved edge is identical to the edge before CaCO_3 units have been removed and hence, the adsorption energies for 100% should be zero. The simulations calculated them to be +16.0 and -1.3 kJ mol^{-1} (Table II), which can thus be taken as a measure of the uncertainty in our calculations and is due to the fact that molecular-dynamics simulations give average energies over a large number of configurations rather than the absolute energy of an energy minimization calculation. Table II shows that removal of the initial calcium carbonate unit from the two steps is energetically reasonably similar for the two surfaces while the energies for any further removals are very different. The major energetic step in the removal process at the obtuse edge is the formation of the initial double-kink sites (25%). The energies of removing of calcium carbonate units from the acute step remain similar throughout the process. The *O* surface shows lower removal energies than the *A* surface at all stages of the process. Thus, under conditions simulating ultra-high vacuum, calcium carbonate removal from the *O* surface should occur preferentially to removal from the *A* surface. This is in accordance with experimental observations that dissolution from the obtuse step is found to be the faster of the two. However, the notion of dissolution in high vacuum is not a sensible one (and calcite growth is usually studied under aqueous conditions). We therefore need to consider the effects of water.

HYDRATED SURFACES

In our previous study of the three calcium carbonate polymorphs⁵² we verified the potential parameters describing the interactions between water molecules and crystal surfaces by showing that without any further refinement of the

TABLE III. Surface energies of hydrated calcite surfaces.

| Surface | Surface energies of hydrated calcite surfaces (Jm^{-2}) | | | | | |
|------------------------------|--|------|------------------|------------------|------|------|
| | 0% | 25% | 50% ^a | 50% ^b | 75% | 100% |
| $A \{3 \bar{1} \bar{4} 8\}$ | 0.22 | 0.27 | 0.32 | 0.35 | 0.32 | 0.22 |
| $O \{3 \bar{1} \bar{2} 16\}$ | 0.60 | 0.65 | 0.65 | 0.67 | 0.63 | 0.60 |

^aAdjacent calcium carbonate units dissolved.

^bAlternating configuration, forming crenellated edge.

model the structure of ikaite, a calcium carbonate hexahydrate, was reproduced well as was the change in enthalpy at 298 K for the dissociation of ikaite to calcite and water. The change in interaction energy for the dissociation of ikaite per water molecule was 47 kJ mol^{-1} agreeing with experimental values of 47 to 50 kJ mol^{-1} .⁵⁵ Although this agreement is fortuitously good it does give us confidence in our reaction energies. As a check on the solution energies we also considered the reaction:



The experimental heat for reaction (3) is $+13 \text{ kJ mol}^{-1}$. We employed molecular-dynamics simulations to estimate this reaction energy. The energies of the aqueous ions were calculated using a simulation cell containing 255 water molecules plus the cation or carbonate group. The simulation cell was equilibrated at NPT and 300 K for 10 000 timesteps of 0.2 femtoseconds after which data were collected for another 50 000 timesteps. Then comparing the average energy of this simulation cell with the energies of the 255 water

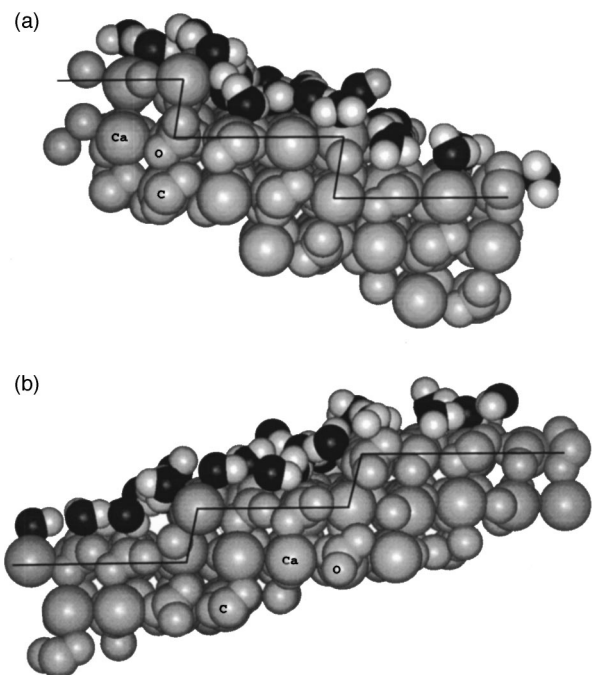


FIG. 2. Different average adsorption patterns at the two hydrated stepped surfaces: (a) A surface and (b) O surface, outlining the steps by a black line. The calcite crystal is shaded pale gray with the different atoms marked and displayed as varying sizes, which are not to scale. The water molecules' oxygen atoms are black and the hydrogen atoms white.

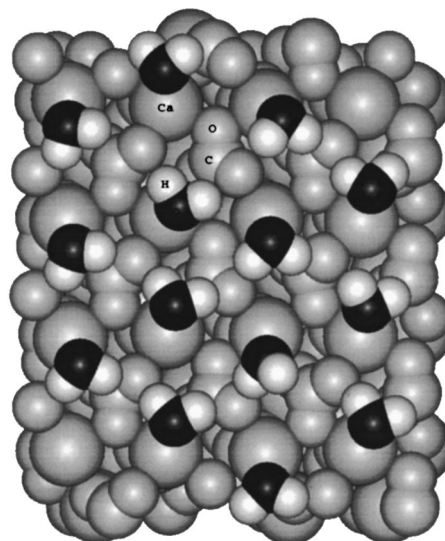


FIG. 3. Plan view of the average structure of the hydrated flat $\{10\bar{1}4\}$ surface, showing a very regular pattern of adsorbed water molecules. (MD simulation at $T=300 \text{ K}$, $t=200 \text{ ps}$).

molecules without the dissolved ion plus the energy of the isolated ion gave the energy of the hydrated ion. Using the above potential parameters we calculated the enthalpy of reaction (3) to be $+33 \text{ kJ mol}^{-1}$. We believe this to be a good agreement, certainly given that this is obtained as an energy difference between very large energies and taking into account the limitations of the atomistic simulation method as described above. In addition, we suggest that the difference of 20 kJ mol^{-1} probably represents the uncertainty in the calculations and could crudely represent the errors in this approach.

In the aqueous simulations the stepped surfaces were covered in a monolayer of water molecules, one per surface calcium atom, which is the preferred configuration for the calcite $\{10\bar{1}4\}$ surface.^{51,52} The surface energies of the hydrated surfaces at the different stages of dissolution are collected in Table III, from which it is evident that the adsorbed water molecules have a stabilizing effect. The surface energies of both surfaces have been lowered by the adsorption of water molecules, with the A surfaces the more stable of the two planes and the most stabilized by the presence of water. Interestingly, the complete step is stabilized to a greater extent than a step containing a kink. Again, as with the dry surfaces, the steps containing complete edges are more stable than the incomplete steps. Figure 2, shows a sideview of the two hydrated steps containing complete edges. It can be seen that due to the different slopes of the two edges the pattern of adsorption of the water molecules is somewhat different on the two steps, even though they both consist of $\{10\bar{1}4\}$ planes. On the planar $\{10\bar{1}4\}$ surface the water molecules adsorb in a regular pattern (Fig. 3), which is disturbed by the presence of the steps, as shown in Fig. 4 which contains plan views of the A and O surfaces with adsorbed water molecules.

The energies of dissolution of calcium carbonate units from the two hydrated surfaces are collected in Table IV. The results show a similar trend to the unhydrated steps, i.e., the dissolution energies for the O surface are lower than for

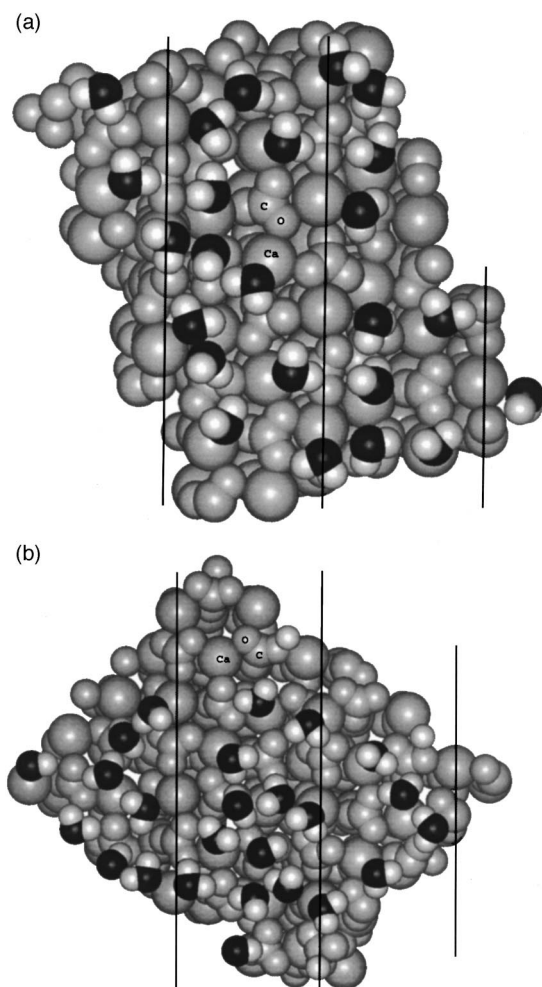


FIG. 4. Plan views of the average structures of the hydrated stepped surfaces showing disruption of the regular adsorption patterns of the water molecules by the step edges, (a) *A* surface and (b) *O* surface. The calcite crystal is shown in pale gray and the steps are indicated by a black line.

the *A* surface. However, the effect is exacerbated by the presence of the water molecules with the double kink on the *O* surface stabilized by 13 kJ mol^{-1} and on the *A* surface destabilized by 35 kJ mol^{-1} . From our calculation of the energy of the reaction defined by Eq. (3) we know that dissolution of a full step edge should release 33 kJ mol^{-1} , which is in good agreement with the values of -29.9 and $-35.0 \text{ kJ mol}^{-1}$ found for the acute and obtuse edge respectively (Table IV) and gives us confidence in the calculated dissolution energies.

TABLE IV. Energies of dissolving calcium carbonate units from hydrated calcite surfaces.

| Surface | Dissolution energies of hydrated calcite surfaces/ CaCO_3 unit dissolved (kJ mol^{-1}) | | | | |
|-------------------------------------|--|------------------|------------------|-------|-------|
| | 25% | 50% ^a | 50% ^b | 75% | 100% |
| <i>A</i> {3 1 $\bar{4}$ 8} | +103.7 | +70.0 | +88.1 | +38.6 | -29.9 |
| <i>O</i> {3 $\bar{1}$ $\bar{2}$ 16} | +45.8 | +6.0 | +21.7 | -19.3 | -35.0 |

^aAdjacent calcium carbonate units dissolved.

^bAlternating configuration, forming crenellated edge.

DISCUSSION

On both surfaces the initial removal of one calcium carbonate unit is the energetically most expensive stage of the dissolution process. However, the aqueous conditions increase the dissolution energies of removing calcium carbonate units from the acute steps selectively. A possible explanation is that the acute surface is much more stable than the obtuse surface and as such not amenable to dissolution, which does fit in with earlier work on magnesium oxide surfaces⁵⁶ that showed that the most unstable surfaces are most reactive. In summary, although the dissolution trend may be the same as the unhydrated surfaces the effect of the solvent is to increase the difference in dissolution energies between the two different steps. This will result in a marked difference in rate of dissolution between the two step edges, as is observed experimentally.^{4,35}

Figure 5 shows a schematic representation of dissolution from the two steps and gives the energies expended or released upon removing a consecutive calcium carbonate unit from the dissolving step, rather than the average adsorption energy given in table IV. As stated above, removal of the first calcium carbonate unit from the acute step of the *A* surface introducing two opposing kink sites on the edge⁵⁴ [Fig. 5(a)], is energetically the most expensive at $+103.7 \text{ kJ mol}^{-1}$. Removing a second unit from the site adjacent to the first, which does not alter the number of kink sites costs much less energy ($+36.2 \text{ kJ mol}^{-1}$). If the energy of removing a portion of the step was constant we would have expected removal of the third unit to cost about another 36 kJ mol^{-1} . However, it is energetically favorable ($-24.1 \text{ kJ mol}^{-1}$).

Alternatively, removal of the second unit from the next nearest neighbor position from the first site introducing yet another double kink site separated by a small gap is, not surprisingly, energetically more expensive than removal from the site next to the first unit ($+72.4 \text{ kJ mol}^{-1}$). This energy is not as large as the formation of an isolated double-kink site ($+103.7 \text{ kJ mol}^{-1}$) indicating that there is an energy of attraction between the double kinks. When finally the fourth calcium carbonate unit is removed, annihilating all kink sites and completing the dissolving edge, a large amount of energy is released, at $-235.4 \text{ kJ mol}^{-1}$ far larger than the energy expended by the removal of the first unit and introduction of the first kink sites.

The process is similar at the obtuse step on the *O* surface [Fig. 5(b)]. The initial removal of the first calcium carbonate unit from the step at $+45.8 \text{ kJ mol}^{-1}$ is not as energetically expensive as from the acute step. When a second unit, adjacent to the first is removed, the energy at $-33.8 \text{ kJ mol}^{-1}$ is exothermic rather than endothermic on the acute surface ($+36.2 \text{ kJ mol}^{-1}$). Removing the second unit from the next nearest-neighbor position and increasing the number of kink sites is energetically still slightly exothermic (-2.4 kJ mol^{-1}). Finally, when the fourth calcium carbonate unit is removed energy is again released ($-82.0 \text{ kJ mol}^{-1}$) although less than on the acute step. On both steps, however, dissolution of the final crystal unit from the dissolving step, and hence creating a complete edge, releases about twice the energy from what is needed to dissolve the first unit from the complete edge (-235.4 vs $+103.7 \text{ kJ mol}^{-1}$ on the acute

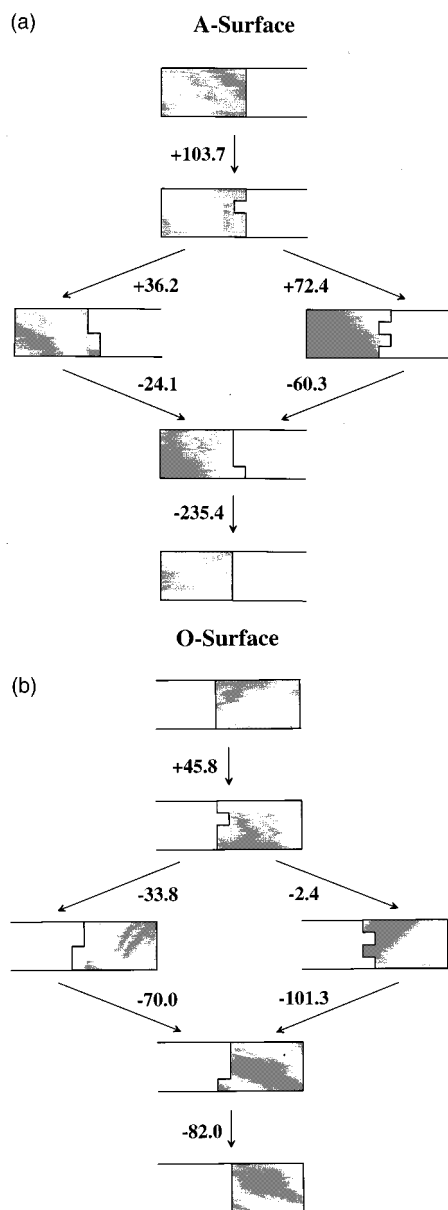


FIG. 5. Schematic representation of the energetics of step-by-step dissolution of calcium carbonate units from (a) the A surface and (b) the O surface.

edge and -82.0 vs $+45.8$ kJ mol^{-1} on the obtuse edge). Therefore, the energy released on dissolution of the final calcium carbonate unit from the edge would be enough to instigate the dissolution of two crystal units from the next step edge.

Thus, the different geometries of the adsorbed water molecules on the two steps play a crucial role in the energetics of dissolution from the step edges. Although the energetically most expensive process of initial dissolution of the first calcium carbonate unit and formation of kink sites is roughly the same for the unhydrated and hydrated O surfaces, hydration of the A surface has made the initial dissolution step much more endothermic. Thus, under aqueous conditions we expect dissolution from the obtuse step to occur preferentially, in agreement with experiment.²⁶ A detailed comparison of the calculations with experiment is difficult since the experimental configuration is not the same as that assumed in

the calculation. However, it is possible to show that the calculated values are not unreasonable in the light of the experimental data.

A considerable amount of data is available on the growth of calcite. Teng *et al.*⁵⁷ have shown that the free-energy change associated with the addition of a new step of length L is given by

$$\Delta g_{\pm} = -(L/b)\Delta\mu + 2c\langle\gamma\rangle_{\pm}, \quad (4)$$

where $\Delta\mu$ is the change of chemical potential per molecule, b is the length of a surface unit cell, and c the width (i.e., the width of a new unit of the growing step). $\langle\gamma\rangle_{\pm}$ are the effective free energies of the steps along the positive and negative $[\bar{4}41]$ and $[48\bar{1}]$ directions. These are given by

$$\langle\gamma\rangle_{+} = (1/4)[2(\gamma_{+} + \gamma_{-}) + (\gamma_{++} + \gamma_{+-})] \quad (5a)$$

$$\langle\gamma\rangle_{-} = (1/4)[2(\gamma_{+} + \gamma_{-}) + (\gamma_{-} + \gamma_{+-})], \quad (5b)$$

where γ_{+} and γ_{-} are the free energies of the $+$ and $-$ steps and γ_{++} , γ_{--} , and γ_{+-} are the contributions to the effective step energies from the corners. The authors⁵⁷ obtained 2.75 eV/nm for $\langle\gamma\rangle_{+}$ and 2.15 eV/nm for $\langle\gamma\rangle_{-}$. The difference between the two gives a value of 0.77 eV/molecule, which is equivalent to $\gamma_{++} - \gamma_{--}$. It is not possible to obtain individual values for the corner energies, however it is clear that the $(++)$ acute angle corner requires much more energy to create than the $(--)$ obtuse angle corner. This is consistent with the results shown bottom to top in Figs. 4(a) and 4(b) where, in the first case, the CaCO_3 unit is placed on the acute angle surface giving a $(++)$ and $(+-)$ corner and in the second case, the unit on the obtuse angle surface gives a $(--)$ and $(+-)$ corner. The difference between these is much larger than experiment (about 1.5 eV/molecule) but the situations are not really comparable since the experiment considers corners at either end of a long step. A better comparison might be to note that the difference $\gamma_{++} - \gamma_{--}$ corresponds to the difference in the creation energy of the two double kink sites (provided that the interactions between the steps across the kink are ignored). This gives an energy of 57.2 kJ mol^{-1} (0.59 eV). This is closer to the experimental result, but all that can be claimed is that the approximate magnitude and sign of the calculation is correct.

Further information can be obtained from the dissolution process. The activation energy for bulk dissolution is 69 ± 12 kJ mol^{-1} (0.72 eV/molecule). This is much larger than the activation energies for pit deepening, 27 ± 5 kJ mol^{-1} (0.28 eV/molecule), or for pit widening, 37 ± 3 kJ mol^{-1} (0.38 eV/molecule).²⁶ Analysis of time-lapse atomic force microscopy experiments on etch pits in dissolving calcite³⁵ gives the step velocities as a function of temperature. This can then be analyzed (either by an analytic treatment using a Terrace-Site-Kink model³⁶ or by kinetic Monte Carlo using a solid-on-solid model³⁷) to give energies for the creation and motion of kinks. The creation of a kink on the slow-moving (acute angled) step costs 0.69 eV (the exact value depends on which model is used to fit the data) and the creation of a kink on the fast-moving step costs 0.67 eV. The corresponding calculated values give 103.7 kJ mol^{-1} (1.07 eV) for the slow step and 45.8 kJ mol^{-1} (0.47 eV) for the fast one. We recall that the estimated error in the calculated values is ± 0.2 eV.

It is not possible to give an estimate of the experimental values beyond the framework of the models, but the fact that the different models give similar values gives some confidence that the values are reasonable. The agreement between theory and experiment is only fair but given the errors, is reasonable.

CONCLUSION

We have employed molecular dynamics simulations to investigate the initial stages of dissolution of calcium carbonate on two stepped calcite surfaces. The surfaces throughout were charge neutral and neutral CaCO_3 units were removed from the surface, implying supersaturation conditions (at low concentrations charged units may desorb). As a result, we can make the following observations:

The calcite $\{3\bar{1}\bar{2}16\}$ surface consisting of $\{10\bar{1}4\}$ planes and obtuse (105°) monatomic steps is less stable than the $\{31\bar{4}8\}$ surface, containing acute (80°) steps, both *in vacuo* and under aqueous conditions.

The dissolution process modelled at the unhydrated

stepped surfaces shows initial and subsequent removal of calcium carbonate units to occur preferentially at the obtuse step edges. Dissolution from the two step edges under aqueous conditions reproduces experimental findings in that dissolution is shown to occur preferentially from the obtuse step. The calculated creation energy of double-kink sites on a growing edge is in approximate agreement with experimental findings, while the calculated dissolution values are similar to those obtained by other models.

In the future we intend to investigate the incorporation of foreign ions such as Mg^{2+} and Li^+ in the calcite crystal and their effect on growth and dissolution. In addition, we aim to employ molecular dynamics simulations to model water adsorption and dissolution at calcite etchpits.

ACKNOWLEDGMENTS

We acknowledge EPSRC and NERC for financial support and thank Molecular Simulations Inc. for the provision of Insight II.

*Electronic address: n.h.deleeuw@bath.ac.uk

†Electronic address: s.c.parker@bath.ac.uk

‡Electronic address: j.harding@ucl.ac.uk

¹D. Beruto and M. Giordani, *J. Chem. Soc., Faraday Trans.* **89**, 2457 (1993).

²C. S. Romanek, E. L. Grossman, and J. W. Morse, *Geochim. Cosmochim. Acta* **56**, 419 (1992).

³S. L. Stipp and M. F. Hochella, *Geochim. Cosmochim. Acta* **55**, 1723 (1991).

⁴N.-S. Park, M.-W. Kim, S. C. Langford, and J. T. Dickinson, *J. Appl. Phys.* **80**, 2680 (1996).

⁵D. Chakraborty and S. K. Bhatia, *Ind. Eng. Chem. Res.* **35**, 1995 (1996).

⁶P. M. Dove and M. F. Hochella, *Geochim. Cosmochim. Acta* **57**, 705 (1993).

⁷W. Dreybrodt, L. Eisenlohr, B. Madry, and S. Ringer, *Geochim. Cosmochim. Acta* **61**, 3897 (1997).

⁸Z. Liu and W. Dreybrodt, *Geochim. Cosmochim. Acta* **61**, 2879 (1997).

⁹R. J. Reeder, J. W. Valley, C. M. Graham, and J. M. Eiler, *Geochim. Cosmochim. Acta* **61**, 5057 (1997).

¹⁰P. Zuddas and A. Mucci, *Geochim. Cosmochim. Acta* **62**, 757 (1998).

¹¹D. Chakraborty, V. K. Agarwal, S. K. Bhatia, and J. Belare, *Ind. Eng. Chem. Res.* **33**, 2187 (1994).

¹²N. Nassralla-Aboukais, A. Boughriet, J. C. Fischer, M. Wartel, H. R. Langelin, and A. Aboukais, *J. Chem. Soc., Faraday Trans.* **92**, 3211 (1996).

¹³J. L. Katz, M. R. Reick, R. E. Herzog, and K. I. Parsiegl, *Langmuir* **9**, 1423 (1993).

¹⁴R. G. Compton and C. A. Brown, *J. Colloid Interface Sci.* **165**, 445 (1994).

¹⁵L. Brecevic, V. Nothig-Laslo, D. Kralj, and S. Popovic, *J. Chem. Soc., Faraday Trans.* **92**, 1017 (1996).

¹⁶M. Deleuze and S. L. Brantley, *Geochim. Cosmochim. Acta* **61**, 1475 (1997).

¹⁷T. Suzuki, S. Inomata, and K. Sawada, *J. Chem. Soc., Faraday Trans. 1* **82**, 1733 (1986).

¹⁸D. S. Cicerone, A. E. Regazzoni, and M. A. Blesa, *J. Colloid Interface Sci.* **154**, 423 (1992).

¹⁹I. Lebrón and D. L. Suárez, *Geochim. Cosmochim. Acta* **60**, 2765 (1996).

²⁰I. Lebrón and D. L. Suárez, *Geochim. Cosmochim. Acta* **62**, 405 (1998).

²¹T. R. S. Wilson and J. Thomson, *Geochim. Cosmochim. Acta* **62**, 2087 (1998).

²²P. R. Kenway, P. M. Oliver, S. C. Parker, D. C. Sayle, T. X. T. Sayle, and J. O. Titiloye, *Mol. Simul.* **9**, 83 (1992).

²³S. C. Parker, E. T. Kelsey, P. M. Oliver, and J. O. Titiloye, *Faraday Discuss.* **94**, 75 (1993).

²⁴S. Rajam and S. Mann, *J. Chem. Soc. Chem. Commun.*, 1789 (1990).

²⁵D. L. Blanchard and D. R. Baer, *Surf. Sci.* **276**, 27 (1992).

²⁶I. N. MacInnes and S. L. Brantley, *Geochim. Cosmochim. Acta* **56**, 1113 (1992).

²⁷J. M. Didymus, P. M. Oliver, S. Mann, A. L. De Vries, P. V. Hauschka, and P. Westbroek, *J. Chem. Soc., Faraday Trans.* **89**, 2891 (1993).

²⁸S. Goni, L. Sobrado, and M. S. Hernandez, *Solid State Ionics* **63**, 786 (1993).

²⁹S. L. Stipp, W. Gutmannsbauer, and T. Lehmann, *Am. Mineral.* **81**, 1 (1996).

³⁰F. Ohnesorge and G. Binnig, *Science* **260**, 1451 (1993).

³¹Y. Liang, A. S. Lea, D. R. Baer, and M. H. Engelhard, *Surf. Sci.* **351**, 172 (1996).

³²A. J. Gratz, P. E. Hillner, and P. K. Hansma, *Geochim. Cosmochim. Acta* **57**, 491 (1993).

³³P. E. Hillner, S. Manne, and P. K. Hansma, *Faraday Discuss.* **95**, 191 (1993).

³⁴N. G. Hemming, R. J. Reeder, and S. R. Hart, *Geochim. Cosmochim. Acta* **62**, 2915 (1998).

³⁵Y. Liang, D. R. Baer, J. M. McCoy, J. E. Amonette, and J. P. LaFemina, *Geochim. Cosmochim. Acta* **60**, 4883 (1996).

³⁶Y. Liang and D. R. Baer, *Surf. Sci.* **373**, 275 (1997).

³⁷J. M. McCoy and J. P. LaFemina, *Surf. Sci.* **373**, 288 (1997).

³⁸M. A. Nygren, D. H. Gay, C. R. A. Catlow, M. P. Wilson, and A.

- L. Rohl, *J. Chem. Soc., Faraday Trans.* **94**, 3685 (1998).
- ³⁹M. Born and K. Huang, *Dynamical Theory of Crystal Lattices* (Oxford University Press, Oxford, 1954).
- ⁴⁰B. G. Dick and A. W. Overhauser, *Phys. Rev.* **112**, 90 (1958).
- ⁴¹A. Pavese, M. Catti, S. C. Parker, and A. Wall, *Phys. Chem. Miner.* **23**, 89 (1996).
- ⁴²T. R. Forester and W. Smith, *DL_POLY user manual* (CCLRC, Daresbury Laboratory, Daresbury, Warrington, UK, 1995).
- ⁴³L. Verlet, *Phys. Rev.* **159**, 98 (1967).
- ⁴⁴S. Nosé, *J. Chem. Phys.* **81**, 511 (1984).
- ⁴⁵W. G. Hoover, *Phys. Rev. A* **31**, 1695 (1985).
- ⁴⁶P. J. D. Lindman and M. J. Gillan, *J. Phys.: Condens. Matter* **5**, 1019 (1993).
- ⁴⁷P. J. Mitchell and D. Fincham, *J. Phys.: Condens. Matter* **5**, 1031 (1993).
- ⁴⁸R. Ferneyhough, D. Fincham, G. D. Price, and M. J. Gillan, *Modell. Simul. Mater. Sci. Eng.* **2**, 1101 (1994).
- ⁴⁹N. H. de Leeuw and S. C. Parker, *Phys. Rev. B* **58**, 13 901 (1998).
- ⁵⁰P. M. Oliver, S. C. Parker, R. G. Egdeell, and F. H. Jones, *J. Chem. Soc., Faraday Trans.* **92**, 2049 (1996).
- ⁵¹N. H. de Leeuw and S. C. Parker, *J. Chem. Soc., Faraday Trans.* **93**, 467 (1997).
- ⁵²N. H. de Leeuw and S. C. Parker, *J. Phys. Chem. B* **102**, 2914 (1998).
- ⁵³W. A. Deer, R. A. Howie, and J. Zussman, *Introduction to the Rock Forming Minerals* (Longham, Harlow, UK, 1992).
- ⁵⁴G. Jordan and W. Rammensee, *Geochim. Cosmochim. Acta* **62**, 941 (1998).
- ⁵⁵J. L. Bischoff, J. A. Fitzpatrick, and R. J. Rosenbauer, *J. Geol.* **101**, 21 (1993).
- ⁵⁶N. H. De Leeuw and S. C. Parker, *Res. Chem. Intermed.* **25**, 195 (1999).
- ⁵⁷H. H. Teng, P. M. Dove, C. A. Orme, and J. J. De Yoreo, *Science* **282**, 724 (1998).